

# Anticancer Properties of N,N-dibenzylasparagine as an Asparagine (Asp) analog, Using Colon Cancer Caco-2 Cell Line

El-Shimaa A. Mohamed<sup>1</sup>, Khalid Bassiouny<sup>1</sup>, Abeer A. Alshambky<sup>1,2</sup>, Hany Khalil<sup>1\*</sup>

## Abstract

**Objectives:** This study was conducted to investigate the potential anticancer properties of N, N-dibenzyl asparagine (NNDAsp), as an Asparagine (Asp) analog, using colon cancer Caco-2 cell and the normal NCM-460 cell line. **Methods:** Cell viability rate and levels of produced lactate dehydrogenase (LDH) were achieved upon treatment with NNDAsp compared to Asp treatment using MTT assay and LDH production kit. The protein expression profile of asparagine synthetase (ASNS) was achieved by using ELISA and flow cytometry assay. The levels of released inflammatory cytokines, including interleukin-1 alpha (IL-1 $\alpha$ ) and IL-1 beta (IL-1 $\beta$ ), were monitored using an ELISA assay. **Results:** Our findings showed significant inhibition of colon cancer cell proliferation accompanied by a high level of produced LDH in a dose-dependent of an NNDAsp treatment without detectable toxic effect in normal cells. Interestingly, NNDAsp showed competitive inhibition of ASNS protein expression, in almost 3% of stained cancer cells, compared to 18% and 35% of untreated cells and cells pre-treated with Asp, respectively. Likewise, the concentration of ASNS protein was dramatically depleted in a dose and time-dependent of NNDAsp treatment in comparison with Asp treatment indicated by ELISA assay. Furthermore, as an apoptotic indicator, the expression of P53 and Caspase 3 (Casp3) was significantly increased in Caco-2 cells treated with NNDAsp at both RNA and protein levels. In contrast, their expression was markedly depleted in Asp-treated cells. In addition, the expression of both IL-1 $\alpha$  and IL-1 $\beta$  was markedly increased in Caco-2 cells in a dose and time-dependent of NNDAsp exogenous treatment. Moreover, targeting of ASNS by the Asp analog, NNDAsp, was further confirmed by the docking analysis of inhibitors ligands and crystal structure of ASNS protein. **Conclusion:** These data provide evidence for the effectiveness of NNDAsp in cancer treatment via selective degradation of ASNS protein expression in colon cancer cells.

**Keywords:** Asparagine-N, N-dibenzyl asparagine- asparagine synthetase- Interleukin 1 $\alpha$

*Asian Pac J Cancer Prev*, 23 (7), 2531-2540

## Introduction

Cell proliferation is one of the most complicated cellular processes that lead to cell division and increasing the copies of each living cell. The mechanisms by which the normal cells can successfully replicate include cyclin-dependent kinases (CDKs), and the epidermal growth factor receptor (EGFR) (Wee and Wang, 2017). The EGFR particularly stimulates downstream targets of the pro-oncoproteins family such as RAS-RAF-MEK-ERK and AKT-PI3K-mTOR signaling pathways (ZHANG and LIU, 2002). In cancer cells, the overexpression of EGFR, and the mutant downstream effectors such as KRAS, BRAF, PIK3CA, P53 and PTEN have been linked to a dynamic change that occurs in cancer cells leading to drug resistance, distinct oncogenicity alteration,

and malignancy transformation (Sobani et al., 2016; Balcik-Ercin et al., 2020). Colon cancer is one of the most commonly diagnosed cancers and a leading cause of cancer death worldwide. More than one million new cases are recognized yearly with a mortality rate of 60% worldwide, of which cancer metastasis is the leading cause of death (Ferlay et al., 2010; Maher et al., 2020). Indeed, one-third of patients with colon cancer have synchronous or metachronous metastasis. The five-year overall survival rate of patients with primary colon cancer was 80–90%, despite being reduced to 40–60% in patients with advanced nonmetastatic tumors and further decreased to 5–10% in patients with metastatic tumors (Wang et al., 2015). Colorectal cancer (CRC) is the type of cancer that starts in the colon or rectum known as bowel cancer or colon cancer (Kim and Chang 2014). Noteworthy, CRC

<sup>1</sup>Department of Molecular Biology, Genetic Engineering and Biotechnology Research Institute, University of Sadat City, 32897 Sadat City, Egypt. <sup>2</sup>Biochemistry Department, Animal Health Research Institute, 33374856 Cairo, Egypt. \*For Correspondence: hany.khalil@gebri.usc.edu.eg

begins like a benign tumor, converted to a malignant tumor invading normal tissue and ultimately migrates all over the body. There are many causes of CRC, including obesity, smoking, lifestyle, aging, inflammatory bowel disease, and genetic syndromes (Durko and Malecka-Panas 2014; Simonian et al. 2018).

The asparagine (Asp) is a crucial amino acid in glycopeptide bonds by stimulating N-glycosyl linkage to the sugar rings. L-asparagine (Asp), analog to L-aspartic acid, is one of the nonessential amino acids with a terminal amine group derived from glutamate in the reaction of glutamine to yield Asp in the presence of ATP (Semsei et al., 1991; Yoo et al., 2020). Typically, asparagine synthetase (ASNS) is an enzyme found in all mammalian organs required to convert glutamine to glutamate and aspartate to Asp-dependent ATP molecules (Lomelino et al., 2017). ASNS protein encoded by a gene located on chromosome 7. Notably, the gene of expression ASNS and its protein profile and activity is highly related to cellular stress and drug resistance mechanism of so many diseases and medical disorders. For instance, in acute lymphoblastic leukemia, elevated ASNS protein level in children is associated with the asparaginase-resistant case during therapy (Chiu et al., 2020). Several studies also indicated the crosslink between elevated ASNS expression and asparaginase efficacy in treating certain solid tumors (Zhang et al., 2014; Lomelino et al., 2017; Jiang et al., 2021). Like other amino acids, Asp plays a crucial role in cancer development as a building block required for protein synthesis (Jiang et al., 2021). Mechanistically, ASNS and Asp inhibit glutamine-depletion-induced endoplasmic reticulum stress in brain cancer cells (Pavlova et al., 2018). In breast cancer cells, Asp can promote epithelial cell proliferation in the disturbance of exogenous glutamine supply (Zhang et al., 2014). Interestingly, evidence indicated the ability of Asp to enhance the expression of glutamine synthetase (GLUL) resulted in increasing glutamine de novo biosynthesis (Pavlova et al., 2018). Therefore, targeting amino acids such as Asp and amino acid synthetase like ASNS has been proved to be helpful pre-clinical therapy in various types of cancer.

The aim of this study was to investigate the potential anticancer properties of N,N-dibenzylasparagine (NNDAsp), as an Asp analog, in colon cancer cell line in-vitro. The cytotoxicity of NNDAsp in the Caco-2 cell line and the normal colon mucosal epithelial cells, NCM-460 cell line, was compared. The expression profile of ASNS was also assessed in response to NNDAsp and Asp treatment to figure out the potential molecular function of NNDAsp as an anticancer agent.

## Materials and Methods

### Cell lines

Colon cancer epithelial cell line Caco-2 cells were kindly provided by (VACSERA, Giza, Egypt). Cells were grown in Roswell Park Memorial Institute (RPMI) 1640 media supplemented with 25 mM HEPS, 4 mM L-glutamine, 4 mM sodium pyruvate, and 10% of heat-treated bovine serum albumin (BSA). The normal human

colon mucosal epithelial cell line (NCM-460 cells) was grown in RPMI media that contains 4 mM L-glutamine and 10% BSA. All cell lines were incubated at 37°C and a relative humidity of 95% (Khalil et al., 2017; Abd El Maksoud et al., 2019a). The cultured cells' imaging was determined using inverted microscopy with a Zeiss A-Plan 10X.

### Preparation of amino acids stocks

To prepare the Asp and NNDAsp in suitable form, 20 mg of each candidate was dissolved in PBS supplemented with 1% DMSO, and different dilutions has been prepared, including 5, 2.5, 1.25 mg/ml of dissolvent buffer. The final extract was incubated at room temperature (R.T.) till used.

### Proliferation assay

To achieve cell proliferation, cells were seeded in triplicate in 96-well plates at 10x10<sup>3</sup> cells per well or in duplicate in a 6-well plate at 10X10<sup>4</sup> cells per well. Cell morphology was assessed using an inverted microscope. The number of living cells was accounted by using a hemocytometer. Accordingly, the old media was removed, and then the cells were washed twice by PBS and trypsinized by adding an appropriate volume of trypsin followed by 3 min incubation at 37°C. Finally, an appropriate volume of complete RPMI media was added to the trypsinized cells, and the number of cells was accounted using the inverted microscope (Taher et al., 2021).

### Cytotoxic concentration 50% (CC50)

The Asp and NNDAsp were tested for their anticancer properties and calculated the potential CC50 in Caco-2 and NCM-460 cells. Therefore, the cells were cultured in triplicate in 96-well plates in a density of 10X10<sup>3</sup>cells/well and were incubated overnight at 37°C and humidity conditions. The cells were treated with different concentrations of each component (20-1.25 mg/ml) followed by overnight incubation. The cell viability rate and cytotoxic concentration were monitored by using MTT colorimetric assay kit (Sigma-Aldrich, Germany). Accordingly, the old media was removed from treated cells seeded in 96-well, and PBS washed the cells, and then 100 µl complete RPMI media was added to each well. Subsequently, 10 µl MTT solution was added to each well, and the plate was incubated for 2 hours at 37°C. Finally, 100 µl SDS-HCl solution was added to each well in the plate which then was incubated for 4 hrs at 37°C. Cell viability was then assessed based on the amount of converted water-soluble MTT to an insoluble formazan which is then solubilized and determined by optical density at 570 nm (El-Fadl et al., 2021).

### Lactate dehydrogenase (LDH) production

LDH assay kit (Abc-65393) was used to assess LDH production in the fluid media collected from cultured-treated cells. According to the manufacturing procedures, 100µl of lysed cells was incubated with 100 µl LDH reaction mix for 30 min at room temperature. A plate reader was used to quantify LDH activity at OD 450 nm.

The relative LDH production is calculated by dividing the mean values of treated cells on the mock values and indicated by fold change (Khalil, 2012; Khalil et al., 2019).

#### *Flow cytometry analysis*

Flow cytometry was used to evaluate the protein expression profile of phosphorylated P53 (Pho-P53), Casp3 and ASNS enzyme in treated Caco-2 cells. Accordingly, drug-treated cells were washed by phosphate buffer saline (PBS) and were trypsinized for 3 min. The complete RPMI medium was added to the trypsinized cells, which were then centrifuged for 3 min at 1500 rpm. The supernatant was discarded, and the pellet was resuspended in PBS for washing and resuspended in PBS with 0.2% formaldehyde for fixation. The cells were resuspended in PBS for permeabilization, including triton-x-100 (0.1%), and incubated for 3 min. For staining of Pho-P53, the cells were resuspended and incubated for 2 hrs at R.T. in the PBS supplemented with 1% BSA and the diluted mouse monoclonal anti-pho-P53 (Sigma-Aldrich, Germany). After washing, the cells were centrifuged and resuspended in the PBS that contains 1% BSA and 1-1000 secondary antibody donkey anti-mouse IgG (Alexa Fluor 594, Invitrogen, Germany). The same conditions were followed in staining of pho-Casp3 protein in treated cells using rabbit polyclonal anti-pho-Casp3 (PromoCell, Germany) and goat anti-rabbit IgG (Alexa Fluor 488, Abcam, USA). For staining ASNS enzyme, the rabbit monoclonal primary antibody (mAb #92479, Cell Signaling Technology, USA) and goat anti-rabbit IgG (Alexa Fluor 488, Abcam, USA) were used. Finally, the flow cytometry assay (BD Accuri 6 Plus) was used to assess the protein levels using a resuspended pellet in 500 µl PBS (Abd El Maksoud et al., 2019b; Hamouda et al., 2021).

#### *Enzyme-linked immunosorbent assay (ELISA)*

Human asparagine synthetase (ASNS) ELISA Kit (AbbeXa, Cambridge, UK) has been used. The microplate provided in this kit has been pre-coated with an antibody specific to ASNS. Standards or samples were then added to the appropriate microplate wells with a biotin-conjugated antibody specific to ASNS. Next, Avidin conjugated to Horseradish Peroxidase (HRP) is added to each microplate well and incubated. After TMB substrate solution was added, only those wells containing ASNS, biotin-conjugated antibody, and enzyme-conjugated Avidin will exhibit color changes. The enzyme-substrate reaction was terminated by adding sulphuric acid solution, and the color change was measured spectrophotometrically at a wavelength of 450 nm +/- 10nm. The concentration of ASNS in the samples is then determined by comparing the O.D. of the samples to the standard curve. ELISA assay was also used to quantify the released interleukin-1α (IL-1α) and IL-1β using human ELISA kits (Abcam 46028 and Abcam 46052, respectively). According to the manufacture protocol, cells cultured in 96-well plates were overnight incubated. Then the cells were treated with different concentrations of each amino acid followed by an incubation period of (0, 6, 12, 24, 36, 48, and 72

hrs). At each time point, the cells were lysed using 1X cell lysis buffer (Invitrogen, USA). Then, 100 µl of the lysed cells were transferred into the ELISA plate reader and incubated for 2 hrs R.T. with 100 µl control solution and 50µl 1X biotinylated antibody. Then 100 µl of 1X streptavidin-HRP solution was added to each well of samples and incubated for 30 min in the dark. 100 µl of the chromogen TMB substrate solution was added to each well of samples and incubated for 15 min at R.T., away from the light. Finally, 100 µl stop solution was added to each well of samples to stop the reaction. The absorbance of each well was measured at 450 nm (Khalil H et al., 2017; Khalil et al., 2020a).

#### *Quantitative real-time PCR (qRT-PCR)*

The quantification analysis of gene expression was detected using qRT-PCR. The total cellular RNA was obtained using TriZol (Invitrogen, USA) and purified using an RNA purification kit (Invitrogen, USA). Complementary DNA (cDNA) was synthesized from 1 µg of total RNA using M-MLV reverse transcriptase (Promega, USA). The P53 and Caspase 3 (Casp3) mRNA expression quantification analyses were achieved using QuantiTect-SYBR-Green PCR Kit (Qiagen, USA) and the specific primers listed in Table 1. The housekeeping glyceraldehyde 3-phosphate dehydrogenase (GAPDH) expression level was used for normalization in the real-time PCR data analysis. The PCR reaction system contained 10 µl SYBR green, 0.25 µl RNase inhibitor (25 U/µl), 0.2 µM of each primer, 2 µL of synthesized cDNA, and nuclease-free water up to a final volume of 25 µL. The following PCR conditions were used; 94°C for 5 min, 35 cycles (94°C for 30 sec, 60°C for 15 sec, 72°C for 30 sec) (Khalil et al., 2019; El-Fadl et al., 2021).

#### *Data analysis*

Microsoft Excel was used to prepare all histograms and charts. Delta-Delta Ct analysis was used in the quantification analysis of mRNA delivered from qRT-PCR assay based on the following equations: (1) delta-Ct = Ct value for gene- Ct value for GAPDH, (2) (delta-delta Ct) = delta Ct value for experimental -delta Ct for control), (3) Quantification fold change = ( 2-delta-delta ct ) (Rao et al., 2013; Khalil et al., 2017). The student's two-tailed t-test was used for statistical analysis. P-value ≤ 0.05 was considered statistically significant.

## **Results**

### *NNDAsp disturbs Caco-2 cell proliferation without affecting NCM-460 cell proliferation*

To test the cytotoxic effect of NNDAsp cell viability rate, MTT assay and relative produced LDH were achieved in Caco-2 and NCM-460 that pretreated with different concentrations of either Asp or NNDAsp. As shown in Figure 1A and Table 2, the mean absorbance values revealed cell viability rate of Caco-2 cells was markedly decreased in a dose-dependent manner of NNDAsp, while showed increasing rate in response to Asp treatment. Interestingly, in both cancer and normal cells, the mean absorbance of treated cells showed constant values in

Table 1. Oligonucleotides sequences used for mRNA Quantification of Indicated Genes

Description	Primer sequences 5'-3'
Casp3-forward	GGACAGCAGTTACAAAATGGATTA
Casp3-reverse	CGGCAGGCCTGAATGATGAAG
P53- forward	GCGAGCACTGCCCAACAACA
P53- reverse	GGTCACCGTCTTGTGTCTCT
GAPDH- forward	TGGCATTGTGGAAGGGCTCA
GAPDH- reverse	TGGATGCAGGGATGATGTTCT

response to Asp and NNDAsp (Figure 1B and Table 2). These findings indicate that NNDAsp can disturb cancer cell proliferation mainly with a cytotoxic concentration of 50% (CC50) with 4 mg/ml. Further, the relative LDH production was significantly increased in cancer cells upon treatment with 4 mg/ml of NNDAsp for 24 hours

compared with untreated cells and cells treated with Triton X-100, as a toxic compound, without detectable cytotoxic effect in normal cells (Figure 1C, Table 3, and Table 4). Together, these data suggest the potential anticancer properties of NNDAsp and further confirm the crucial role of Asp in cell proliferation.

*NNDAsp affects cancer cell morphology and the number of survived cells*

Cell morphology and the number of survived cells were assessed in both treated cells with Asp and NNDAsp using an inverted microscope. Markedly, the cell morphology revealed a disturbing proliferation of Caco-2 cells treated with 4 mg/ml NNDAsp compared with the cell morphology of other treated cells (Figure 2A). The number of surviving cells significantly decreased in response to NNDAsp treatment only in colon cancer cells. At the same time, the same concentration of Asp

Table 2. Cell Viability Rate of Treated Caco-2 Cells

Treatment	Concentration (mg/ml)	Mean Absorbance (570nm)		P-values	
		NCM-460 cells	Caco-2 cells	NCM-460 cells	Caco-2 cells
Asp	0.0 <sup>‡</sup>	0.57±0.1	0.57±0.1		
	1.25	0.70±0.06	0.70±0.06	> 0.05	> 0.05
	2.5	0.80±0.11	0.84± 0.11	< 0.05*	< 0.05*
	5	0.74±0.1	0.89± 0.08	< 0.05*	< 0.01**
	10	0.86±0.08	0.89± 0.06	< 0.01**	< 0.01**
	20	0.89±0.07	1.01± 0.02	< 0.01**	< 0.01**
NNDAsp	0.0 <sup>‡</sup>	0.65±0.13	0.6± 0.13		
	1.25	0.58±0.1	0.60± 0.13	> 0.05	> 0.05
	2.5	0.5±0.1	0.48± 0.13	> 0.05	> 0.05
	5	0.54±0.08	0.23± 0.1	> 0.05	< 0.01**
	10	0.64±0.13	0.12± 0.1	> 0.05	< 0.01**
	20	0.74±0.13	0.08± 0.02	> 0.05	< 0.01**

‡, DMSO; \*, Indicates significant P values ≤ 0.05; \*\*, Indicates high significant P values ≤ 0.01

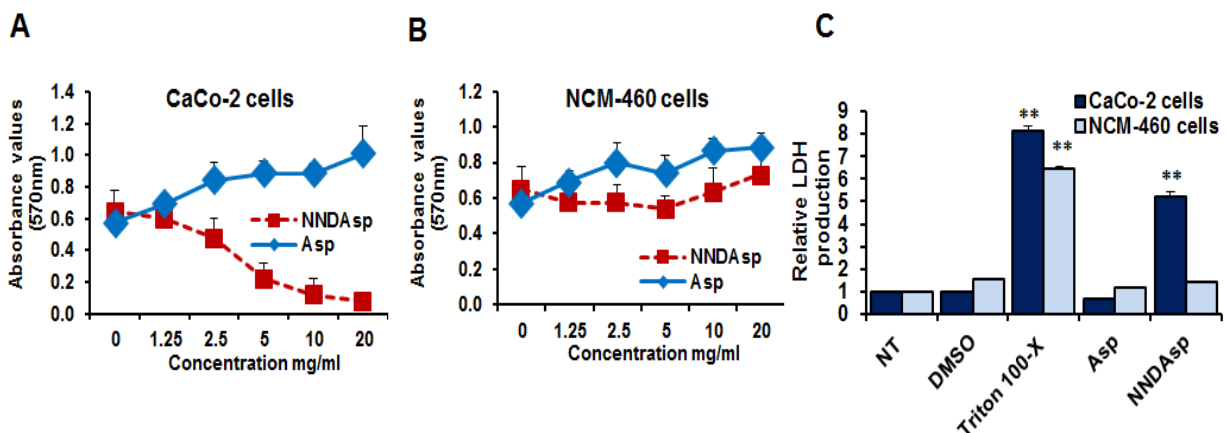


Figure 1. Cell Viability and Cytotoxic Effect of Asp and NNDAsp Treatment. (A) Cell viability rate of Caco-2 cells that were pretreated with indicated concentrations of either Asp or NNDAsp for 24 hrs compared with DMSO (0 concentration). (B) Cell viability rate of NCM-460 cells that were pretreated with the same concentration of Asp or NNDAsp for 24 hrs compared with DMSO (0 concentration) using MTT assay. (C) Relative LDH production from treated cells compared to Triton 100-X treated cells and untreated cells (N.T.). Error bars indicate the S.D. of four different replicates. The student's two tails t-test was used to determine the significance of differentiated values. (\*) indicates P-values ≤ 0.05, and (\*\*) indicates the P ≤ 0.01.

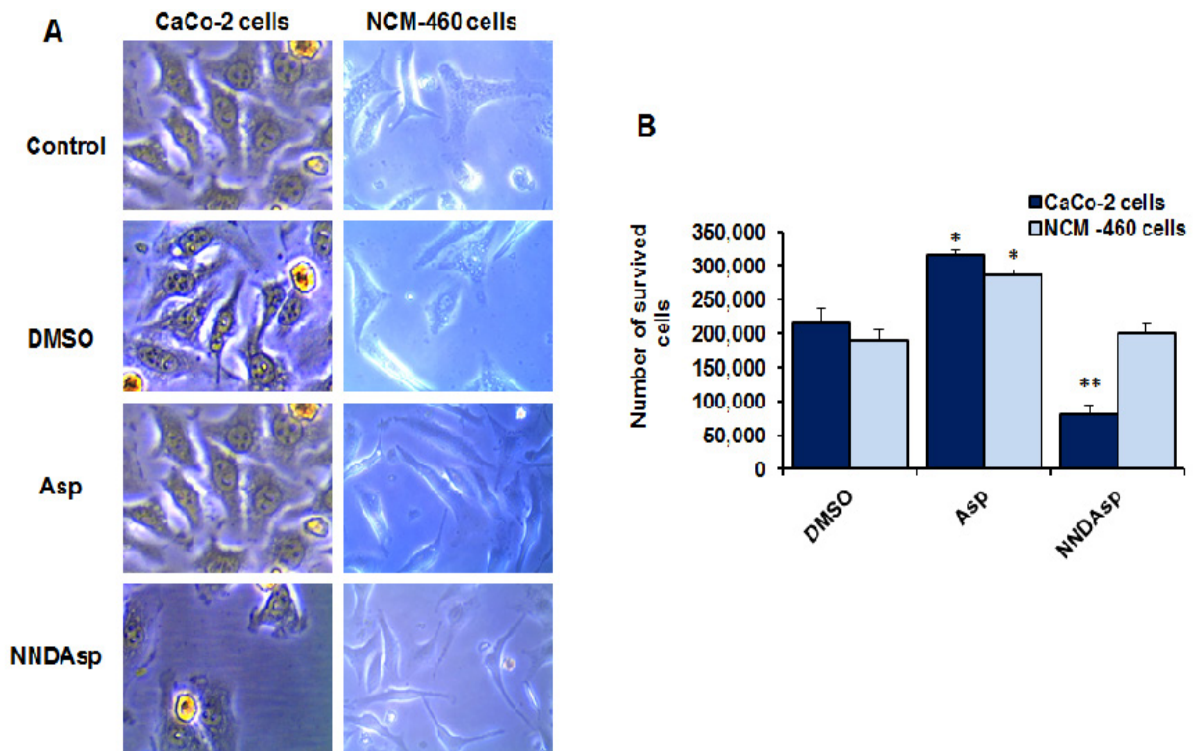


Figure 2. Cell Survival and Morphology in Response to Asp and NNDAsp Treatment. (A) Representative cell morphology indicated by inverted microscopy reveals cell viability of both Caco-2 cells and NCM-460 cells that were pretreated with 250 µg/ml of Asp and NNDAsp for 24 hrs. (B) The number of survived cells upon treatment with indicated compositions. Error bars indicate the standard deviation (S.D.) of three independent experiments. The student's two tails t-test was used to determine the significance of differentiated values. (\*) indicates P-values  $\leq 0.05$ , and (\*\*) indicates the P  $\leq 0.01$ .

showed an increasing number of survived cells (Figure 2B and Table 5). These findings indicate the severe effect of NNDAsp treatment in the Caco-2 cells. In contrast,

Asp treatment stimulates cell proliferation without any detectable toxic effect.

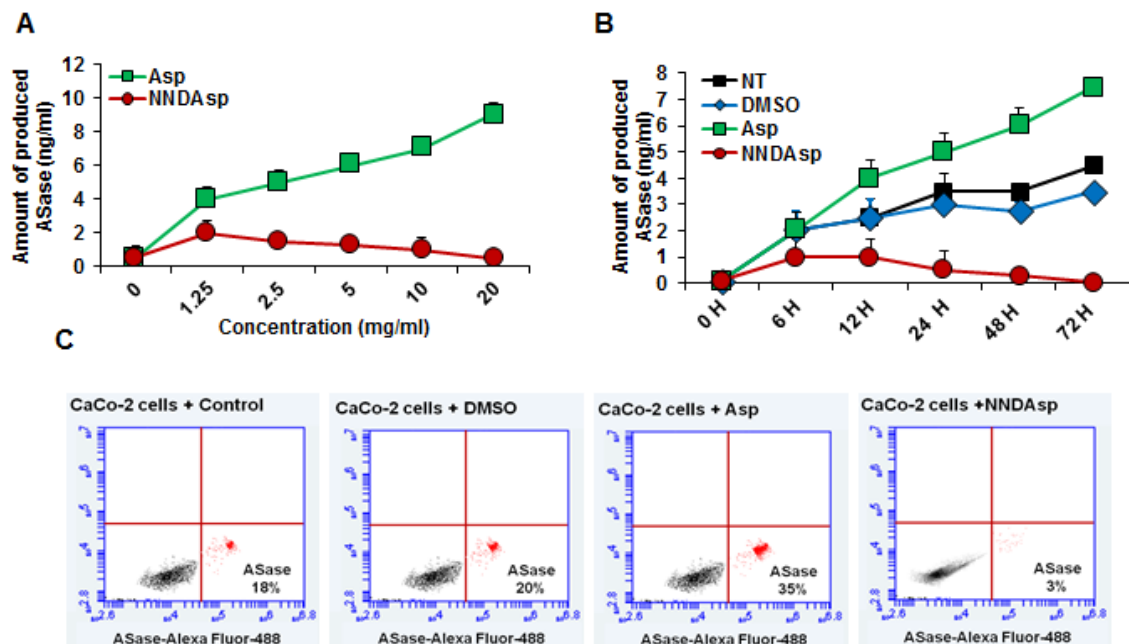


Figure 3. Expression Profile of P53 and Casp3 as Apoptosis Regulators. (A) Quantification of the mRNA expression level of the P53 gene indicated by fold change in treated Caco-2 cells compared with untreated cells (N.T.) and DMSO-treated cells. (B) The mRNA expression level of Caps3 gene was quantified as indicated by fold change in treated Caco-2 cells compared with untreated cells (N.T.) and DMSO-treated cells. Error bars indicate the S.D. of two independent experiments. The student's two tails t-test was used to determine the significance of differentiated Ct values. (\*) indicates P-values  $\leq 0.05$ , and (\*\*) indicates the P  $\leq 0.01$ .

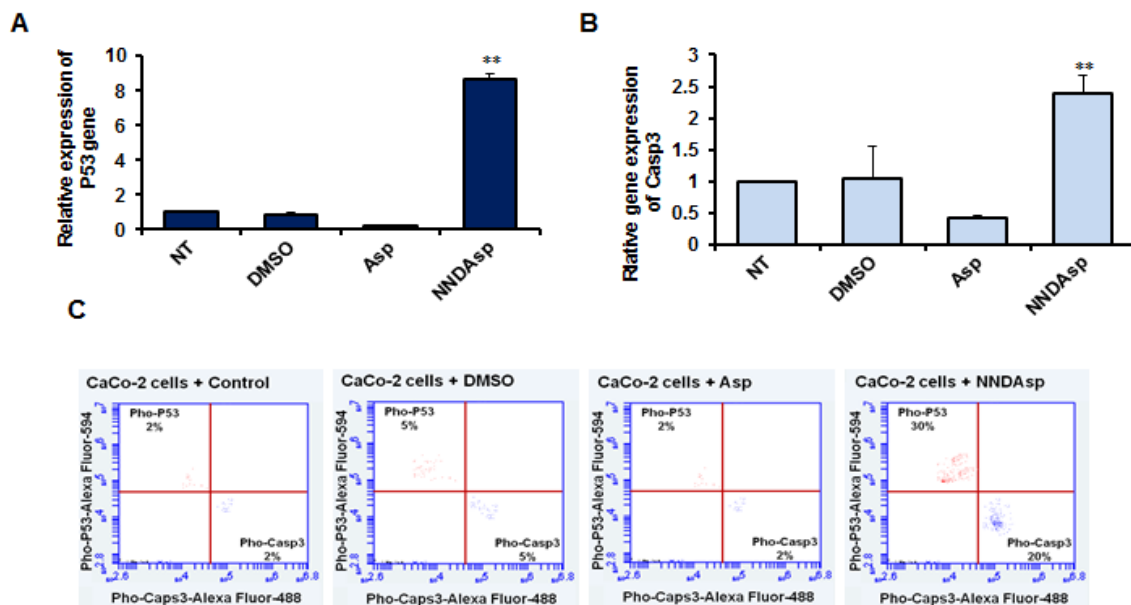


Figure 4. Expression Profile ASNS Protein in Amino Acid-Treated Cells. The concentration of ASNS (pm/ml) in Caco-2 cells treated with different concentrations of each amino acid for 24 hrs compared with DMSO-treated cells. (B) The concentration of ASNS (pm/ml) in Caco-2 cells treated with 4 mg/ml of each amino acid and incubated for the indicated time point, DMSO-treated cells served as control treatment. Error bars reveal the S.D. of three replicates. (C) Flow cytometry fractionation quantifies the kinetic profile of ASNS protein expression in Caco-2 cells treated with 4 mg/ml of each amino acid compared to DMSO treated cells.

Table 3. LDH Production in Treated Cancer Cells (Caco-2 Cells)

	NT	DMSO	Triton 100-X	Asp	NNDAsp
Mean absorbance	0.05±0.01	0.05±0.01	0.4±0.27	0.03±0.02	0.26±0.02
Relative LDH production	1	0.98	8.1	0.69	5.23
P values		0.91	0.04*	0.26	0.05*

NT, Untreated cells (Control)

*NNDAsp stimulates programmed cell death of treated colon cancer cells*

To confirm the cooperation of NNDAsp in cancer cell death, the expression profile of P53, as a tumor suppressor gene, and Casp3, as an indicator for apoptotic signaling, was monitored in treated Caco-2 cells at both RNA and

protein levels. Expectedly, the relative expression of both P53 and Casp3 was dramatically unregulated, at the RNA level, in cells treated with NNDAsp compared to control cells and cells treated with Asp (Figure 3A and B). The statistical analysis presented in Table 7 indicated that the upregulation of P53 and Casp3 gene

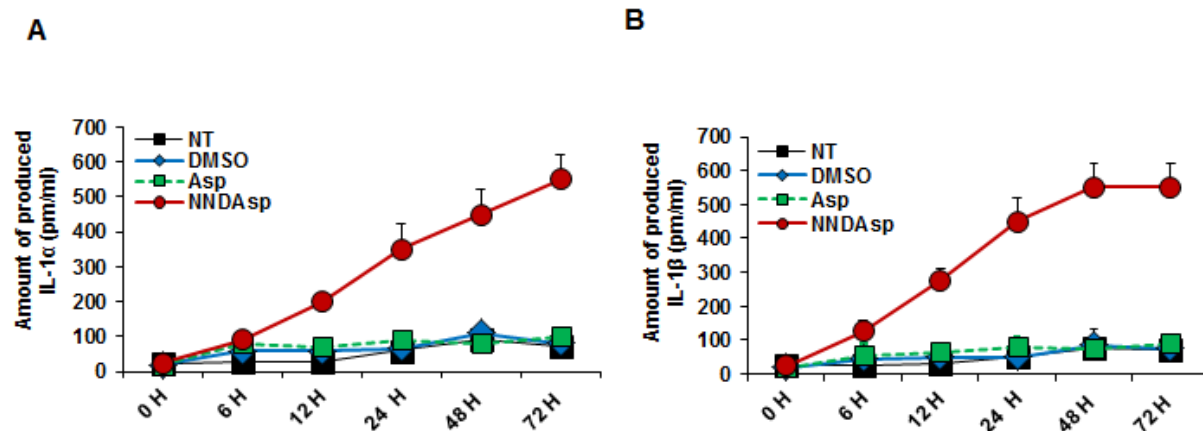


Figure 5. Levels of Produced Inflammatory Interleukins in Treated Cells. The concentration of produced IL-1α (pm/ml) in the fluids media of Caco-2 cells that were subjected to 4 mg/ml of each amino acid at the indicated time points compared with DMSO-treated cells. (B) Level of produced IL-1β (pm/ml) from Caco-2 cells that were subjected to 4 mg/ml of each amino acid for the indicated time points compared with DMSO-treated cells. Error bars reveal the S.D. of three replicates.

Table 4. LDH Production in Treated Normal Cells (NCM-460 cells)

	NT	DMSO	Triton 100-X	Asp	NNDAsp
Mean absorbance	0.04±0.01	0.06±0.03	0.27±0.03	0.05±0.01	0.06±0.02
Relative LDH production	1	1.6	6.5	1.2	1.44
P values		0.14	0.001**	0.37	0.77

Table 5. Number of Survived Cells Upon Treatment

	DMSO		Asp		NNDAsp	
	NCM-460 cells	Caco-2 cells	NCM-460 cells	Caco-2 cells	NCM-460 cells	Caco-2 cells
Mean	190000 ±14142	215000 ±21213	285000 ±7071	315000 ±7071	200000 ±14142	80000 ±1412
P values			0.014*	0.02*	0.55	0.01**

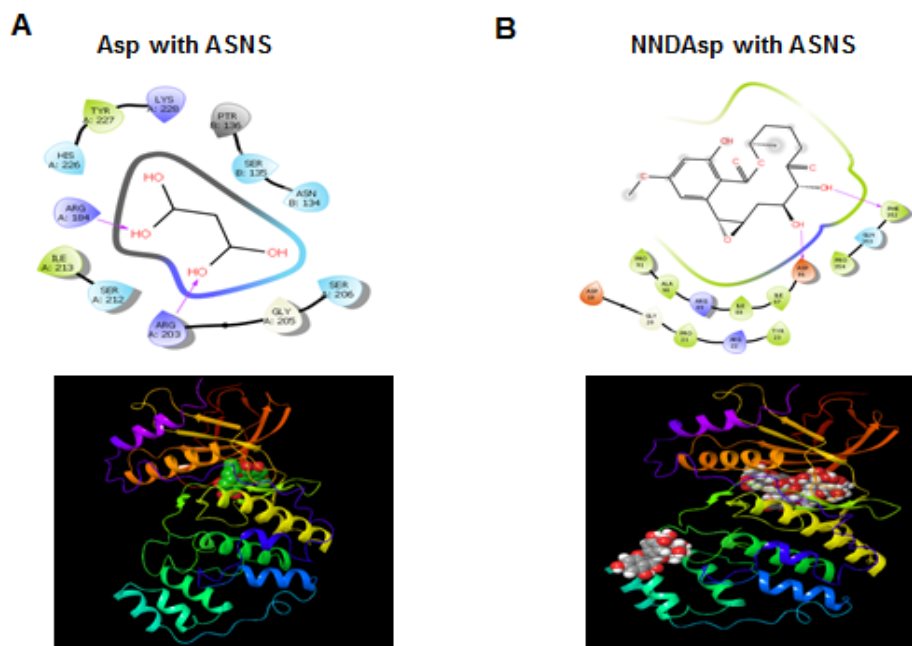


Figure 6. Binding Discrimination of Amino Acid Ligands with ASNS Protein. (A and B) The pharmacophore mapping snapshot indicates the possible hydrophobic interaction and binding affinity between Asp, NNDAsp, respectively, and the ASNS chain protein crystal structure.

expression was highly significant since P values were equal to 0.002 and 0.01, respectively. Furthermore, flow cytometry was used for quantification of phos-P53 and Casp-3 proteins at a single-cell level via a combination of specific primary antibodies to stain treated cells. To quantify the corresponding proteins profile in treated cells, the percentage of positive events was correlated to the

Table 6. Quantification Analysis of P53, and Casp3 Gene Expression in Caco-2-Treated Cells

Genes	Treatment	Expression fold changes	P-values
P53	NT	1.00±0.00	
	DMSO	0.8±0.17	> 0.05
	Asp	0.18±0.07	> 0.05
	NNDAsp	8.6±0.26	< 0.01**
Casp3	NT	1.00±0.00	
	DMSO	1.04±0.5	> 0.05
	Asp	0.42±0.04	> 0.05
	NNDAsp	2.37±0.03	< 0.05*

relative fluorescent intensity of the Alexa Fluor signal of secondary antibodies. Interestingly, the kinetic expression profile of both phos-P53 and Casp3 proteins was markedly increased more up to 20%, while their kinetic expression was strongly decreased less than 5% of stained-control cells and cells treated with Asp (Figure 3C). Together, these data suggest that NNDAsp can restore the expression of P53 and stimulate the expression of Casp3 TET3 in both RNA and protein levels to produce programmed cells death in treated cells (PCD) in infected cells.

*NNDAsp regulates the expression profile of ASNS enzyme in a time and dose-dependent manner*

To address the connection of amino acids treatment and the expression profile of ASNS protein in treated cells, ASNS protein expression was measured in different time points and various concentrations upon treatment using ELISA assay. Compared with Asp, NNDAsp treatment showed a potent reduction of ANSN protein concentration in a time and dose-dependent manner (Figure 4A and B). Furthermore, the quantification analysis of ASNS protein

expression using flow cytometric assay showed a potent reduction of ASNS protein expression, less than 5%, in stained Caco-2 cells treated with 4 mg/ml NNDAsp. While showed more than 18% in control cells, 19% in DMSO-treated cells, and 35% in cells treated with the same concentration of Asp (Figure 4C). Collectively, these findings proved the targeting of ASNS protein by NNDAsp in a time and dose-dependent manner in the treated Caco-2 cell line.

#### *NNDAsp stimulates IL-1 $\alpha$ and IL-1 $\beta$ expression in colon cancer cells*

To determine the correlation between NNDAsp treatment and produced inflammatory cytokines from treated cells, IL-1 $\alpha$  and IL-1 $\beta$  were measured in a time-course experiment using ELISA assay. Interestingly, NNDAsp treatment showed a high production level of both IL-1 $\alpha$  and IL-1 $\beta$  in a time-dependent manner. In contrast, the production level of both interleukins was dramatically reduced in treated cells with Asp and control-treated cells (Figure 5A and B). Together, these data further confirm the impact of NNDAsp in regulating the production of proinflammatory cytokines from treated cells and reveal its ability to stimulate PCD in colon cancer cells.

#### *Binding Based-Cross Docking Analysis of Asp and NNDAsp Ligands and ASNS crystal structure*

The docking analysis presented in Figure 6 reveals that the ASNS protein residues ARG 184 and ARG 203 formed a hydrogen bond with an Asp ligand molecule (A). Meanwhile, PHE 352 and ASP 86 in ASNS protein formed hydrogen bonds with the NNDAsp molecule (B). These results indicate the possible interaction and direct interference of NNDAsp and Asp with ASNS protein in treated cells.

## **Discussion**

The role of ASNS and amino acids in hallmarks of tumor malignancy has been reported in several studies (Kuo et al., 2021; Wei et al., 2021). In the current work, we investigated the molecular influence of NNDAsp, as a modified amino acid, in the proliferation attitude of colon cancer Caco-2 cells compared to normal human colon mucosal epithelial cells (NCM-460 cells). NNDAsp demonstrated the ability to induce PCD in colon cancer cells via rescue P53 and Caps3 gene expression in treated cells. Significantly, NNDAsp reduced the expression profile of the ASNS enzyme, which is responsible for the generation of aspartate and glutamate and contributes to the drug resistance mechanism during cancer therapy. Our findings provide evidence for the potential anticancer properties of NNDAsp with minimal cytotoxic outcomes in normal cells.

During the imbalanced availability of amino acids, the ASNS gene is targeted by two signaling pathways to ensure cell survival: the Unfolded Protein Response (UPR) (Kilberg et al., 2009) and the Amino Acid Response (AAR) (Kilberg et al., 2012). Under the endoplasmic reticulum (ER) stress and through the activation of the PKR-like ER (PER) and GCN2 protein

kinases, both UPR and AAR pathways converge on the phosphorylation of the  $\alpha$ -subunit of the initiation factor eIF2. Subsequently, the eIF2 effector provokes the depletion of global protein synthesis and the translation of selected mRNAs, including the ATF4 transcription factor. Noteworthy, ATF4 is a crucial trans-activator for ASNS induction by binding to an enhancer element within the ASNS promoter (Balasubramanian et al., 2013). Recent evidence demonstrated the translational reprogramming in ASNS-depleted cancer cells that depends on the increase of the MAPK-interacting kinase 1 (MNK1) and eukaryotic translation initiation factor 4E (eIF4E), resulting in increasing ATF4 translation and ASNS expression (Pathria et al., 2019). Additionally, ASNS transcription is also affected negatively by other factors like P53, a tumor suppressor gene (Chiu et al., 2020). Likewise, we hypothesized that NNDAsp treatment could negatively regulate ASNS protein expression in colon cancer cells via direct interaction with its synthetase sites. As a negative correlation, the depletion of ASNS by NNDAsp in colon cancer cells activated the expression of P53 and stimulated the programmed cell death in treated cells. The human ASNS enzyme includes the C-terminal domain, similar to ASNS in other organisms, and the N-terminal glutaminase domain. The glutaminase domain has a topology like other amidotransferases. In addition, the amino acids in the synthetase site are, for the most part, conserved in human and bacterial ASNS. Also, other preserved amino acid residues are recognized in the interface of ASNS domains (Zhu et al., 2019). Indeed, we identified two binding sites at the N-terminal domain of the ASNS enzyme by which NNDAsp binds with amino acid residues; phenylalanine and asparagine indicated by docking analysis. Accumulating evidence showed the association between Raf/MEK/ERK signaling and the expression of Asp biosynthesis enzyme ASNS, demonstrating the sensitivity of melanoma and pancreatic cancer cells to Asp depletion, resulting in disturbing cancer cell proliferation (Pathria et al., 2019). Also, ASNS depletion has been reported to inhibit the panel of breast cancer, prostate cancer, and melanoma cell profanation (Pathria et al., 2019). Notably, the mitogen-activated protein kinase (MAPK), including Raf/MEK/ERK pathway, serves as a critical signal transducer of receptor tyrosine kinases. The Ser/Thr kinase Raf protein (c-Raf-1, Raf-B, or Raf-A) activates the downstream kinase MEK1 and MEK2, which, in turn, phosphorylate Ser/Thr kinases ERK1 and its homolog ERK2 (Shaul and Seger, 2007; Elimam et al., 2020). The Raf/MEK/ERK pathway regulates cell survival, cell cycle progression, and differentiation. Furthermore, the Raf/MEK/ERK pathway can also modulate the activity of many proteins involved in the apoptotic signal, such as Bim, Bax, Casp-9, Casp-3, and P53, which, in turn, regulate cellular autophagy and result in PCD (McCubrey et al., 2007; Khalil et al., 2020b; El-Fadl et al., 2021).

Collectively, our findings further proved ASNS as an attractive candidate to prevent cancer proliferation and stimulate the expression of the tumor suppressor gene, P53, which in turn activates apoptotic signaling in colon cancer cells.

In conclusion, the expression of ASNS in cancer cells is increased to fill the cell need for Asp, which cooperates in many biological processes related to cell proliferation and cancer development. Thus targeting Asp by asparaginase is affected in cancer therapy; however, ASNS expression was linked to the asparaginase-resistant mechanism during therapy. Therefore, this study demonstrates that NNDAsp, an Asp analog, can disrupt colon cancer cell proliferation without affecting the normal human colon mucosal epithelial cell line. NNDAsp successfully induced PCD in cancer-treated cells by restoring P53 gene expression and regulating apoptotic signaling in treated cells. Importantly, our findings proved that NNDAsp targets ASNS enzyme indicated by ELISA assay and flow cytometric analysis in the Caco-2 cell line.

Docking analysis confirmed the possible interaction and binding affinity between NNDAsp and ASNS protein domain structure. Furthermore, NNDAsp stimulates the production level of proinflammatory cytokines IL-1 $\alpha$  and IL-1 $\beta$  that facilitate the PCD in cancer-treated cells. Together, these data suggested that NNDAsp is an attractive agent that can regulate colon cancer cell proliferation without detectable toxic effects in normal cells and indicating the potential role of NNDAsp indirectly to overcome the asparaginase-resistant mechanism during cancer therapy.

## Author Contribution Statement

El-Shimaa Salah and Abeer Alshambky provided the experiments and helped in writing the manuscript. Khalid Bassiouny helped in supervision and data analysis. Hany Khalil designed the research plan, supervised overall research, provided and interpreted data and wrote the manuscript.

## Acknowledgments

### Funding statement

This work is a part of a master thesis and is personally funded by the authors.

### Ethical statement

This study was approved by the ethical committee of Genetic Engineering and Biotechnology Research Institute, University of Sadat City, Egypt.

### Availability of data and materials

The data supporting this study's findings are available from the corresponding author upon reasonable request.

### Conflicts of interest

All authors declare that there are no conflicts of interest.

## References

Abd El Maksoud AI, Taher RF, Gaara AH, et al (2019a). Selective regulation of B-Raf dependent K-Ras/Mitogen-Activated protein by natural occurring multi-kinase inhibitors in cancer cells. *Front Oncol*, **9**, 1220.

- Abd El Maksoud AI, Taher RF, Gaara AH, et al (2019b). Selective Regulation of B-Raf Dependent K-Ras/Mitogen-Activated Protein by Natural Occurring Multi-kinase Inhibitors in Cancer Cells. *Front Oncol*, **9**, 1220.
- Balasubramanian MN, Butterworth EA, Kilberg MS (2013). Asparagine synthetase: regulation by cell stress and involvement in tumor biology. *Am J Physiol Metab*, **304**, 789–99.
- Balcik-Ercin P, Cetin M, Yalim-Camci I, Uygur T, Yagci T (2020). Hepatocellular Carcinoma Cells with Downregulated ZEB2 Become Resistant to Resveratrol by Concomitant Induction of ABCG2 Expression. *Mol Biol*, **54**, 75–81.
- Chiu M, Taurino G, Bianchi MG, Kilberg MS, Bussolati O (2020). Asparagine Synthetase in Cancer: Beyond Acute Lymphoblastic Leukemia. *Front Oncol*, **9**, doi:10.3389/fonc.2019.01480.
- Durko L, Malecka-Panas E (2014). Lifestyle Modifications and Colorectal Cancer. *Curr Colorectal Cancer Rep*, **10**, 45–54.
- El-Fadl HMA, Hagag NM, El-Shafei RA, et al (2021). Effective Targeting of Raf-1 and Its Associated Autophagy by Novel Extracted Peptide for Treating Breast Cancer Cells. *Front Oncol*, **11**, 3317.
- Elimam H, El-Say KM, Cybulsky AV, Khalil H (2020). Regulation of Autophagy Progress via Lysosomal Depletion by Fluvastatin Nanoparticle Treatment in Breast Cancer Cells. *ACS Omega*. doi:10.1021/acsomega.0c01618.
- Ferlay J, Shin HR, Bray F, Forman D, Mathers C, Parkin DM (2010). Estimates of worldwide burden of cancer in 2008: GLOBOCAN 2008. *Int J Cancer*, doi:10.1002/ijc.25516.
- Hamouda RA, Abd El Maksoud AI, Wageed M, et al (2021). Characterization and Anticancer Activity of Biosynthesized Au/Cellulose Nanocomposite from *Chlorella vulgaris*. *Polymers (Basel)*, **13**.
- Jiang J, Batra S, Zhang J (2021). Asparagine: A Metabolite to Be Targeted in Cancers. *Metabolites*, **11**, 402.
- Khalil H (2012). Influenza A virus stimulates autophagy to undermine host cell IFN- $\beta$  production. *Egypt J Biochem Mol Biol*, **30**, 283–99.
- Khalil H, Abd El Maksoud AI, Alian A, et al (2020a). Interruption of Autophagosome Formation in Cardiovascular Disease, an Evidence for Protective Response of Autophagy. *Immunol Invest*, **49**, 249–63.
- Khalil H, Abd El Maksoud AI, Roshdey T, El-Masry S (2019). Guava flavonoid glycosides prevent influenza A virus infection via rescue of P53 activity. *J Med Virol*, **91**, 45–55.
- Khalil H, Abd Elhady A, Elawdan K, et al (2020b). The mechanical autophagy as a part of cellular immunity; Facts and Features in treating the medical disorders. *Immunol Invest*, doi:10.1080/08820139.2020.1828453.
- Khalil H, El Malah T, El Maksoud AIA, et al (2017). Identification of novel and efficacious chemical compounds that disturb influenza A virus entry in vitro. *Front Cell. Infect Microbiol*, doi:10.3389/fcimb.2017.00304.
- Khalil H, Arfa M, El-Masrey S, EL-Sherbini S, Abd-Elaziz A (2017). Single nucleotide polymorphisms of interleukins associated with hepatitis C virus infection in Egypt. *J Infect Dev Ctries*, **11**, 261–8.
- Kilberg MS, Balasubramanian M, Fu L, Shan J (2012). The Transcription Factor Network Associated With the Amino Acid Response in Mammalian Cells. *Adv Nutr*, **3**, 295–306.
- Kilberg MS, Shan J, Su N (2009). ATF4-dependent transcription mediates signaling of amino acid limitation. *Trends Endocrinol Metab*, **20**, 436–43.
- Kim ER, Chang DK (2014). Colorectal cancer in inflammatory bowel disease: The risk, pathogenesis, prevention and diagnosis. *World J Gastroenterol*, doi:10.3748/wjg.v20.i29.9872.

- Lomelino CL, Andring JT, McKenna R, Kilberg MS (2017). Asparagine synthetase: Function, structure, and role in disease. *J Biol Chem*, **292**, 19952–8.
- Maher E, Gedawy G, Fathy W, et al (2020). Hsa-miR-21-mediated cell death and tumor metastases: A potential dual response during colorectal cancer development. *Middle East J Cancer*, **11**, doi:10.30476/mejc.2020.83146.1139.
- McCubrey JA, Steelman LS, Franklin RA, et al (2007). Targeting the RAF/MEK/ERK, PI3K/AKT and p53 pathways in hematopoietic drug resistance. *Adv Enzyme Regul*, **47**, 64–103.
- Pathria G, Lee JS, Hasnis E, et al (2019). Translational reprogramming marks adaptation to asparagine restriction in cancer. *Nat Cell Biol*, **21**, 1590–1603.
- Pavlova NN, Hui S, Ghergurovich JM, et al (2018). As Extracellular Glutamine Levels Decline, Asparagine Becomes an Essential Amino Acid. *Cell Metab*, **27**, 428–38.
- Rao X, Huang X, Zhou Z, Lin X (2013). An improvement of the  $2^{-\Delta\Delta CT}$  method for quantitative real-time polymerase chain reaction data analysis. *Biostat Bioinforma Biomath*, doi:10.1016/j.micinf.2011.07.011. In: *Innate*.
- Shaul YD, Seger R (2007). The MEK/ERK cascade: From signaling specificity to diverse functions. *Biochim Biophys Acta Mol Cell Res*, doi:10.1016/j.bbamcr.2006.10.005.
- Simonian M, Khosravi S, Mortazavi D, et al (2018). Environmental Risk Factors Associated with Sporadic Colorectal Cancer in Isfahan, Iran. *Middle East J Cancer*, **9**, 318–22.
- Sobani ZA, Sawant A, Jafri M, Correa AK, Sahin IH (2016). Oncogenic fingerprint of epidermal growth factor receptor pathway and emerging epidermal growth factor receptor blockade resistance in colorectal cancer. *World J Clin Oncol*, **7**, 340–51.
- Taher RF, Al-Karmalawy AA, Abd El Maksoud AI, et al (2021). Two new flavonoids and anticancer activity of *Hymenosporum flavum*: in vitro and molecular docking studies. *J Herbmед Pharmacol*, **10**, 443–58.
- Wang J, Du Y, Liu X, Cho WC, Yang Y (2015). MicroRNAs as Regulator of Signaling Networks in Metastatic Colon Cancer. *Biomed Res Int*, **2015**, 823620.
- Wee P, Wang Z (2017). Epidermal Growth Factor Receptor Cell Proliferation Signaling Pathways. *Cancers (Basel)*, **9**, 52.
- Zhang J, Fan J, Venneti S, et al (2014). Asparagine plays a critical role in regulating cellular adaptation to glutamine depletion. *Mol Cell*, **56**, 205–18.
- ZHANG W, LIU HT (2002). MAPK signal pathways in the regulation of cell proliferation in mammalian cells. *Cell Res*, **12**, 9–18.
- Zhu W, Radadiya A, Bisson C, et al (2019). Author Correction: High-resolution crystal structure of human asparagine synthetase enables analysis of inhibitor binding and selectivity. *Commun Biol*, **2**, 438.



This work is licensed under a Creative Commons Attribution-Non Commercial 4.0 International License.